INVESTIGATIONS ON THE INFLUENCE OF A FORMING GAS ANNEAL ON THE MECHANICAL PROPERTIES OF THE PRINTED AG THICK FILM FRONT SIDE CONTACT OF SOLAR CELLS AFTER COFIRING

S. Ohl [1], G. Schubert [2], J. Horzel [3], Giso Hahn [1]
[1] University of Konstanz, Department of Physics, D-78457, Germany
phone: +49 7531 883730, fax: +49 7531 883895, Sibylle.Ohl@uni-konstanz.de
[2] Sunways AG, Macairestr. 3-5, D-78467 Konstanz, Germany
[3] Schott Solar GmbH, Carl-Zeiss-Str. 4, D-63755 Alzenau, Germany

ABSTRACT: The beneficial effect of a forming gas anneal (FGA) in hydrogen atmosphere on the fill factor (FF) of screen printed solar cells has been shown previously [1, 2]. In this contribution the effect of a FGA on the mechanical properties of the silver printed front side contact of solar cells is investigated for most relevant wafer surfaces (mc, Cz, EFG, each flat as well as textured). In particular, the adhesion of the busbar to the surface of the silicon wafer is examined by using standardized pull test conditions after soldering pre-soldered Cu-ribbons onto the busbars of the solar cells. It was found that the FGA has no significant influence on the mechanical properties of the busbars including the adhesion strength. Samples which experienced higher than optimal firing conditions show slightly higher adhesion strength and a wider distribution of the forces needed to detach the busbar.
Keywords: Annealing, Contact, Manufacturing and Processing, Adhesion, Solder, Interconnect

1 INTRODUCTION

Nakajima at al. [1] showed that the annealing of the fired contact in a hydrogen atmosphere at around 400 °C improves the contact resistance. The FGA enhances the fill factor (FF) and range of favorable firing conditions and offers the possibility to increase FF and efficiency after cell processing using non-optimal firing conditions (in particular for over-fired contacts).

Furthermore, the FGA improves the contact quality of high-sheet-resistance emitters [2]. Recently, it was found that a forming gas anneal can improve the contact resistance of a silver thick film contact even to n-type emitters with a low surface concentration of about $N_{D,surface} = 5x10^{19}$ cm^{-3} (sheet resistance > 60 Ohm/sq) and might therefore be useful for future cell concepts including drive-in emitters [3].

The chemical reactions during a forming gas anneal presumably lead to a reduction of metal oxides in the glass by hydrogen, and the number and size of metallic precipitates is enhanced [3]. This raises the question whether the glass layer gets more porous and therefore more likely to give in under mechanical stress occurring e.g. when interconnecting Si solar cells in solar module strings.

2 EXPERIMENTAL SET UP

2.1 Sample processing

Most relevant wafer surfaces were included in the test; three groups of each 80 solar cells with a size of 12.5 x 12.5 cm^2 were produced:

- Multi-crystalline (mc) wafers: flat and acidic textured (thickness after processing approx. 220 – 230 µm)
- CZ: flat (180 µm) and alkaline textured (240 – 250 µm)
- EFG (Edge-defined Film-fed Growth): flat and acidic textured (approx. 300 µm)

The solar cells were fabricated in a typical industrial processing sequence (40 – 50 Ohm/sq emitter, PECVD SiNx, ARC, screen printed Al backside, Ag frontside contacts with commercially available lead containing Ag paste, used as the standard paste at the University of Konstanz. The cells were fired under a) optimal firing conditions and b) over-fired conditions (mc and Cz: + 40 K, EFG: + 30 K) in a typical industrial conveyor belt furnace.

Subsequently, the groups were split each into two subgroups, one group was processed with a FGA (forming gas anneal) for 30 min at 400°C in an argon-hydrogen (10%) atmosphere, one group without anneal as reference.

2.2 Electrical characterization

IV-measurements were performed before and after the FGA for all cells to obtain an electrical characterization. The results of the IV-characterization where the following:

- Fill factor improvement for overfired flat mc: mean FF increases from 76.1% to 77.8% after anneal. (Maximal FF mc_{flat} after anneal: 78.3%, maximal FF improvement 3.7%.)
- Fill factor improvement for overfired textured mc: the mean FF increased from 76.5% to 77.0% after anneal. (Maximal FF mc_{tex} after anneal: 78.3%.)
- The fill factor of the flat and the textured fired with optimal firing conditions did not improve significantly after the anneal. (The maximal FF was 78.4% for flat mc and 77.7 for textured mc after anneal.)
- No fill factor improvement was measured for C_Z / EFG cells. A possible explanation might be the high fill factor already achieved without anneal for those cells, as a FGA will not improve very good contacts. (Max. FF of over-fired C_Z-cells before anneal up to 80.1% for flat cells (mean: 79.4%) and 79.3% for textured cells (mean: 78.1%); FF for over-fired EFG cells before anneal up to 75.1% for flat cells (mean: 73.4%), up to 76.2% for textured cells (mean: 75.2%).) At the same time it might be possible that the process window for the firing parameter was larger than expected and the firing temperature for overfiring was too low.

2.3 Soldering of the Cu-ribbon

Cu-interconnection ribbons were soldered onto the busbars. Two different methods were applied for each subgroup:

a) Semi-automatic: the solar cells were soldered in a tabber-stringer on front and back side, Cu-ribbons (2.0 mm x 0.1 mm) plated with 20-30 µm SnAg (3.5% Ag) were used. Four separate solder connections were made for each busbar with a length of 1 cm to 2.5 cm each.

b) Manual: the solar cells were put on an aluminum plate heated to 100°C and the ribbon was soldered with a soldering iron at a temperature of 350°C onto the entire busbar. The copper interconnection ribbon was manufactured by Schlenk with a composition typical for industrial module production (19.5 µm L-SN62Pb36Ag2, 1.6 mm x 0.15 mm). Flux IF 2005 M was used to treat the ribbon and the busbar surfaces, no additional solder was used. Only the front side of the cells was tabbed, the backside remained without ribbons.

On each side at the edge of the wafer about 4 cm of the ribbon was standing out and was used to be attached to the pulltester described below.

2.4 Pulltesting

To test the mechanical stability of the silver contact a pulltester developed at the University of Konstanz was used. (This tool is commercially available via GP Solar GmbH, GP STAB-TEST/PRO.)

The pulltester has a step motor and is moving the force-measurement-unit in upward direction with constant speed. The sample was mounted beneath the moving unit at an angle of 45° [4]. The soldered ribbon was bent and inserted into a fixture. The cell was hold down on both sides of the busbar at a distance of approx. 1 mm to the ribbon to minimize flexure of the wafer during the pulling process.

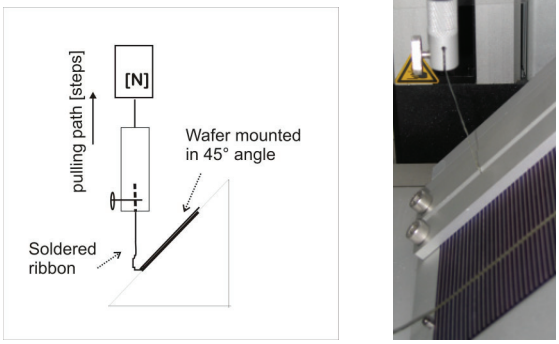

Figure 1: Pulltester used for experiments

The path of the force-unit and the measurement force is collected in a data file.

3 ANALYSIS

3.1 Typical failure modes

We assume that the typical stack of a soldered busbar is made of (from top to bottom layer) Cu-ribbon, solder, the bulk of the silver metallization consisting of sintered Ag particles, a glass layer, and silicon. The forces needed to destroy this bond depend on multiple factors. The effects of the firing parameters, the metallization composition, and the print parameters (and others) have been investigated before e.g. by Whittle et al. [4]. The analysis of the points of fractures for different wafer types led us to distinguish between four typical adhesive failure modes:

a) failure within the solder itself or not soldered to the ribbon at all
b) rupture in the glass layer
c) rupture in the bulk of the silver busbar (metallization)
d) fracture of the silicon

3.2 Optical / SEM / EDX analysis

Figure 2 shows a typical force vs. pulling distance diagram with the related photograph of the detached busbar. Point A shows the end of the tapering of the busbar. Points B are fractures of the busbar in the silicon. In region C different types of failure are present.

The typical classes defined before could be found on each investigated sample independent of the firing or post metallization treatment. In Figure 3 to 5 typical SEM/EDX results are shown for the points of fracture in the glass or in the metallization respectively (see figure 2, point C).

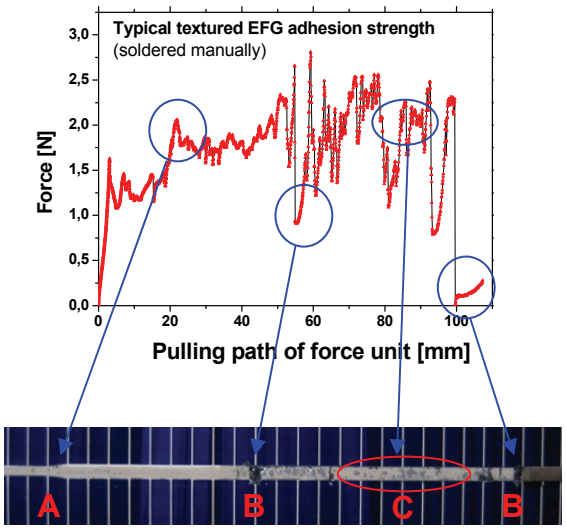

Figure 2: Photograph of the busbar of a texured EFG wafer in combination with the force vs. path diagram. Point A: end of busbar tapering; points B: fracture of the busbar the silicon; point C: different type of failures

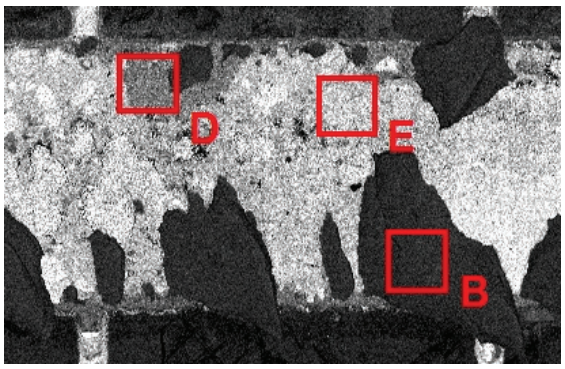

Figure 3: Typical composition mode SEM picture of busbar. Point B: fracture in the silicone substrate; point D: fracture in the glass; point E: fracture in the bulk of the silver metallization

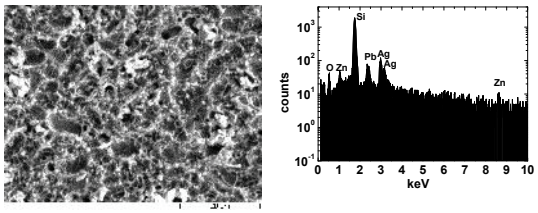

Figure 4: SEM & EDX analysis of failure as in region of point D (fracture in glass); the structure of acidic texturing covered by a glass layer is visible

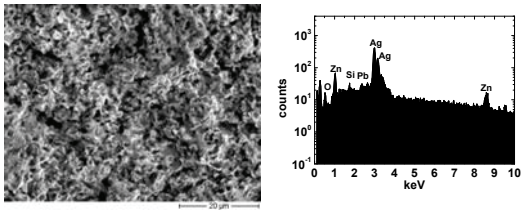

Figure 5: SEM & EDX analysis of failure as in region of point E (fracture in metallization); the typical porous structure of sintered Ag particles is visible

3.3 Statistics

As the wafer is mounted at an angle of 45° and not moving in horizontal direction while the force measurement unit is moving in upward direction, the angle between ribbon and wafer decreases during the pull test. Therefore the measured force depends on the pulling path. We decided not to correct the measured values as the influence decreases with increasing pulling distance.

In some cases less data points than usual were collected, depending on the capacity utilization of the measurement computer. Thus, we interpolated the raw data in order to obtain equidistant data points which would enable further statistical analysis (e.g. in form of histograms).

As it is difficult to distinguish between measurement artifacts (for example when the pre-soldered Cu-ribbon is straightened) and actual forces leading to failures, the recorded force values were cut off below a threshold for further statistical data analysis. Additionally only areas in which dissociation of the busbar bond took reliably place were taken into account and the data between the soldering areas were cut off from further analysis. The data of the semi-automatically soldered cells were taken from a pulling distance of 5 mm, this is the distance when the ribbon is usually fully straightened and the pulling forces begin to act on the busbar bond. All data points below 0.5 N were excluded as the force for the path between the four solder points does not reach exactly zero and the solder areas have not all the same length.

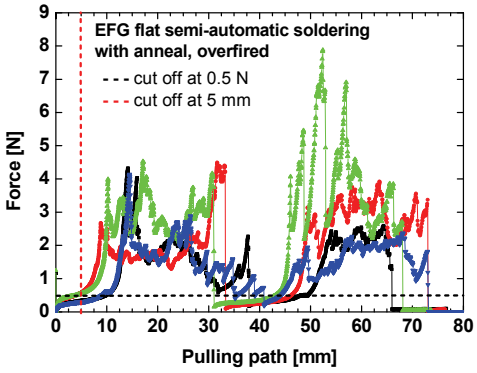

Figure 6: Force vs. path diagram for flat EFG cells soldered semi-automatically

The data of manually soldered cells were taken only from a pulling distance of 23 mm as the busbar has a V-shaped form and the soldered area decreases at the border of the wafer. All force values below 0.3 N were excluded.

A display of the data as histogram (number of data points versus force) is useful to describe the force distribution as it is shown in figure 7. This plot displays the distribution of the measured adhesive strength: for the adjusted data of the curve in figure 2. The mean value of the force is 1.7 N. 90% of all values below the mean value are above 1.0 N, 90% of all values above the mean value are below 2.3 N.

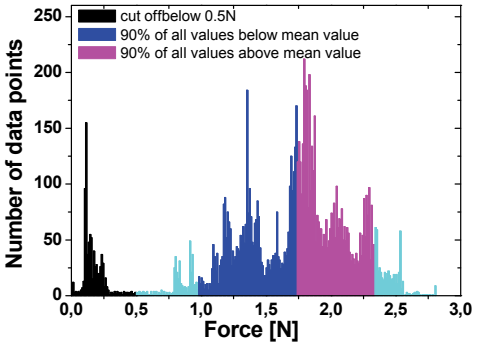

Figure 7: Histogram for one datafile (textured EFG, see figure 2)

For each of the six groups of cells (mc, Cz, EFG; each flat and textured) the data for all samples with the same processing parameters (anneal / no anneal, standard fire temperature / overfired) were used to extract mean value, 90% criterion, standard deviation, median, and maximum force.

4 RESULTS OF STATISTICAL ANALYSIS

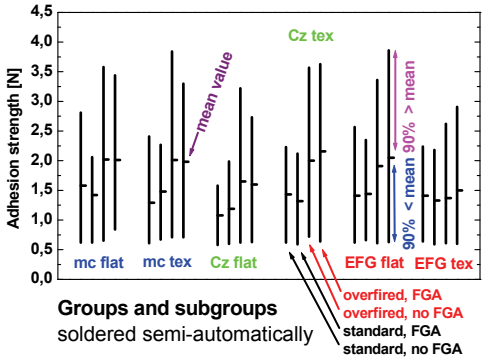

Figure 8: Mean value and upper & lower 90% for all groups soldered semi-automatically

For semi-automatically soldered processing, the overfired samples show a slightly higher mean value and a wider distribution of the adhesion strength for all groups. No significant difference in adhesion strength has been noticed when comparing groups without or with FGA (figure 8).

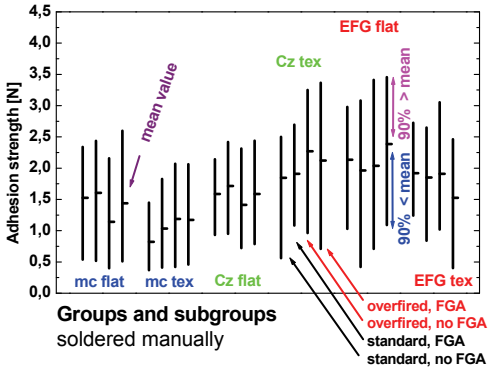

Figure 9: Mean value and upper & lower 90% for all groups soldered manually

The groups soldered manually show a tendency for a more narrow adhesion strength distribution and the difference between groups processed with standard firing parameters and overfired samples is not as significant as for the automatically soldered cells (figure 9). This could be an indication for the less reliable technique of manual soldering compared to semi-automatic soldering. The results for all cells are summarized in table 1 and table 2.

Table 1: Mean value, median and standard deviation for all cells soldered semi-automatically

material	process (semi-auto.)	Mean force [N]	Median force [N]	std dev
mc flat	FGA overfired	2.0	1.9	0.7
	FGA standard	1.4	1.5	0.4
	overfired	2.0	1.9	0.8
	standard	1.6	1.6	0.7
mc tex	FGA overfired	2.0	1.9	0.7
	FGA standard	1.5	1.5	0.5
	overfired	2.0	1.9	0.9
	standard	1.3	1.2	0.5
Cz flat	FGA overfired	1.6	1.5	0.7
	FGA standard	1.2	1.1	0.4
	overfired	1.6	1.6	0.8
	standard	1.1	1.1	0.3
Cz tex	FGA overfired	2.2	2.1	0.9
	FGA standard	1.3	1.3	0.4
	overfired	2.0	1.9	0.8
	standard	1.4	1.4	0.5
EFG flat	FGA overfired	2.1	2.0	0.9
	FGA standard	1.4	1.4	0.5
	overfired	1.9	1.9	0.8
	standard	1.4	1.3	0.6
EFG tex	FGA overfired	1.6	1.5	0.7
	FGA standard	1.3	1.3	0.5
	overfired	1.4	1.4	0.6
	standard	1.4	1.4	0.5

Table 2: Mean value, median and standard deviation for all cells soldered manually

material	process (manual)	Mean force [N]	Median force [N]	std dev
mc flat	FGA overfired	1.4	1.4	0.7
	FGA standard	1.6	1.7	0.6
	overfired	1.1	1.1	0.5
	standard	1.5	1.5	0.5
mc tex	FGA overfired	1.2	1.1	0.5
	FGA standard	1.0	1.0	0.4
	overfired	1.2	1.2	0.5
	standard	0.8	0.8	0.3
Cz flat	FGA overfired	2.1	2.2	0.8
	FGA standard	1.9	1.9	0.4
	overfired	2.3	2.3	0.7
	standard	1.8	1.9	0.5
Cz tex	FGA overfired	1.6	1.6	0.5
	FGA standard	1.7	1.7	0.4
	overfired	1.4	1.4	0.5
	standard	1.6	1.6	0.4
EFG flat	FGA overfired	2.4	2.4	0.7
	FGA standard	2.0	2.0	0.8
	overfired	2.0	2.2	0.7
	standard	2.1	2.2	0.5
EFG tex	FGA overfired	1.5	1.6	0.6
	FGA standard	1.9	1.9	0.5
	overfired	1.9	1.8	0.6
	standard	1.9	1.9	0.5

5 CONCLUSIONS

While improving the process window, the application of the FGA was not found to influence the mechanical properties of the silver thick film contact for all investigated samples. However, the effect of a higher firing temperature became apparent. Overfired samples show a slightly higher mean value and a wider distribution of the adhesion strength.

6 ACKOWLEDGEMENTS

We would like to thank Axel Herguth for many hours of discussion as well as scientific and technical support. Thanks to Daniel Reinke for support in data processing.

7 REFERENCES

[1] T. Nakajima, A.Kawakami, A. Tada, Int. J. Hybrid Microelectronics 6 (1) (1983) 580-586
[2] Hilali et al., Journal of the Electrochemical Society, 152 (10) G742-G749 (2005)
[3] G. Schubert et al., Proceedings 21st European Photovoltaic Solar Energy Conference (2006), page 1460
[4] B.R. Whittle at al., Proceedings 21st European Photovoltaic Solar Energy Conference (2006), page 1243